Evaluating Brain Anatomical Correlations via Canonical Correlation Analysis of Sulcal Lines

Pierre Fillard, Xavier Pennec, Paul M. Thompson, Nicholas Ayache

INRIA

INSTITUT NATIONAL DE RECHERCHE EN INFORMATIQUE ET EN AUTOMATIQUE

Evaluating Brain Anatomical Correlations via Canonical Correlation Analysis of Sulcal Lines

Pierre Fillard — Xavier Pennec — Paul M. Thompson — Nicholas Ayache

N° 6241

June 2007

Thème BIO

ISSN 0249-6399 ISRN INRIA/RR--6241--FR+ENG

Evaluating Brain Anatomical Correlations via Canonical Correlation Analysis of Sulcal Lines

Pierre Fillard* , Xavier Pennec* , Paul M. Thompson† , Nicholas Ayache*

Thème BIO — Systèmes biologiques
Projet Asclepios

Rapport de recherche n° 6241 — June 2007 — 12 pages

Abstract: Modeling and understanding the degree of correlations between brain structures is a challenging problem in neuroscience. Correlated anatomic measures may arise from common genetic and trophic influences across brain regions, and may be overlooked if structures are modeled independently. Here, we propose a new method to analyze structural brain correlations based on a large set of cortical sulcal landmarks (72 per brain) delineated in 98 healthy subjects (age: 51.8 +/-6.2 years). First, we evaluate the correlation between any pair of sulcal positions via the total covariance matrix, a 6×6 symmetric positive-definite matrix. We use Log-Euclidean metrics to extrapolate this sparse field of total covariance matrices to obtain a dense representation. Second, we perform canonical correlation analysis to measure the degree of correlations between any two positions, and derive from it a p-value map for significance testing. We present maps of both local and long-range correlations, including maps of covariation between corresponding structures in opposite hemispheres, which show different degrees of hemispheric specialization. Results show that the central and inferior temporal sulci are highly correlated with their symmetric counterparts in the opposite brain hemisphere. Moreover, several functionally unrelated cortical landmarks show a high correlation as well. This structural dependence is likely attributable to common genetic programs, experience-driven plasticity, and coordinated brain growth or presence of anatomical links (neural fibers).

Key-words: correlation, Log-Euclidean, variability, tensor, brain, computational anatomy

* INRIA Sophia Antipolis - Asclepios Project - France
† Laboratory of Neuro Imaging, Dept. of Neurology, UCLA School of Medicine

Unité de recherche INRIA Sophia Antipolis
2004, route des Lucioles, BP 93, 06902 Sophia Antipolis Cedex (France)
Téléphone : +33 4 92 38 77 77 — Télécopie : +33 4 92 38 77 65

Evaluation des Corrélations Anatomiques du Cerveau via l'Analyse des Corrélations Canoniques des Lignes Sulcales

Résumé : La modélisation et la compréhension du degré de corrélations entre les structures du cerveau est un problème important en neurosciences. Des facteurs génétiques et trophiques communs à différentes régions du cerveau peuvent être responsables de mesures anatomiques corrélées, et peuvent être manquées si l'on modélise les structures indépendemment les unes des autres. Ici, nous proposons une nouvelle méthode d'analyse des corrélations structurelles du cerveau en se basant sur une grand nombre de repères corticaux , les sillons (72 par cerveau), delinéés chez 98 sujets sains (age: 51.8 +/-6.2 ans). Premièrement, nous évaluons les corrélations entre chaque paire de positions sulcales via la matrice de covariance totale, une matrice 6×6 symétrique et définie-positive. Nous utilisons les métriques Log-Euclidienne pour extrapoler ce champ épars de matrices de covariance totales pour obtenir une représentation dense. Deuxièmement, nous effectuons l'analyse des corrélations canoniques pour mesurer le degré de corrélations de ces deux positions, et nous dérivons de cette analyse une carte de p-value pour tester la significativité du résultat. Nous présentons des cartes de corrélations locales mais également à longue distance, ce qui comprend des cartes de co-variation entre structures correspondantes dans les deux hémisphères, montrant des degrés différents de spécialisation hémisphérique. Les résultats montrent que les sillons central et temporel inférieur sont fortement corrélés avec leur équivalent symétrique dans l'autre hémisphère. Par ailleurs, plusieurs repères corticaux à priori non-reliés au niveau fonctionnel montrent une forte corrélation. Cette dépendence structurelle est probablement due à des programmes génétiques communs, une neuro-plasticité guidée par l'expérience, une croissance du cerveau coordonnée ou bien la présence de liens anatomiques (fibres nerveuses).

Mots-clés : corrélation, Log-Euclidien, variabilité, tenseur, cerveau, anatomie algorithmique

1 Introduction

Understanding structural correlations between brain structures is a challenging problem in neuroscience. Most computational anatomic studies of development and disease study deficits or changes by modeling individual brain structures independently, or create voxel-based maps of group anatomical differences. This reveals factors (e.g., age or disease) that influence each brain structure individually, but may miss important supra-regional correlations, such as brain regions that develop or fail to develop together, or correlations between structures in opposite brain hemispheres. Mechelli et al. [1] discovered (1) spatial correlations of the gray matter density between corresponding regions in opposite brain hemispheres, except in the visual cortex, and (2) some negative correlations between functionally distinct regions in the same hemisphere. Neuroscientists are interested in identifying the reasons of such long-range brain correlations, and what causes them at a genetic and environmental level. Normally coordinated systems may be disrupted in neuropsychiatric disorders such as schizophrenia, autism, and Williams syndrome, and systems with known fiber or functional connectivity are thought to exert mutual influences on each other's growth, via activation-dependent plasticity. Structures in different lobes also influence each other's degeneration, for instance when loss of neuronal input from one brain region induces degeneration in another. Despite many hypotheses, few tools allow such long-range correlations to be measured, and thus studied empirically.

An efficient, parsimonious model of the complex patterns of brain correlations should help to identify factors that influence them. Inter-hemispheric correlations (i.e., correlations between point in anatomically homologous structures in both hemispheres) are of interest as they shed light on how their functions become specialized or depend on each other. Improved modeling of correlations of brain structures could make it easier to isolate specific effects of genetic polymorphisms on these normal correlations. Furthermore, information on statistical correlations could reduce the difficulty of automated segmentation and labeling of brain structures. Accessing anatomical correlations also opens up a broad range of studies and comparing groups (e.g., disease versus normal) and a new path to generate hypotheses regarding patterns of brain growth.

We have previously built first-order models (mean anatomical templates), and second-order models (variability models) [2] of the sulcal lines to capture the 3D variations of each anatomical point independently around a mean cortex anatomy, after registration of multi-subject anatomical images to a common reference space. These variations are often represented by covariance matrices, or variability tensors, as variations may not be the same in all directions. Here, we go one step further and model the joint variability of all pairs of anatomical points, to see how the displacement of any point in a specific subject w.r.t. a reference anatomy covaries with the displacement of neighboring or distant point (e.g., anatomically homologous regions in the opposite hemisphere).

In Section 2, we introduce the main tool of our analysis: the total covariance matrix (TCM) between two vector variates, and we recall how to extract from it some matrix and scalar measures to test if these two variables are correlated. In Section 3, we experiment this framework on TCMs defined from anatomical landmarks (sulcal curves). We start by

studying the TCMs of 6 sulcal positions to the rest of the brain, which eventually lead us to analyze the TCMs of all sulcal positions of one hemisphere with their homologous positions in the opposite hemisphere.

2 The Total Covariance Matrix

2.1 Definition

Let $X = \{X_i\}_{i=1..N}$ and $Y = \{Y_i\}_{i=1..N}$ be the sets of N measures of two random vectors whose dimensionality is d. Computing the correlation between X and Y requires to know not only the variability of each vector (i.e., its covariance matrix), but also their cross-covariance. We therefore define the TCM of X and Y that contains this information as $\Lambda(X,Y)$:

$$\Lambda(X,Y) = \frac{1}{N-1}\sum_{i=1}^{N} \begin{pmatrix} X_i - \bar{X} \\ Y_i - \bar{Y} \end{pmatrix} \begin{pmatrix} X_i - \bar{X} \\ Y_i - \bar{Y} \end{pmatrix}^{\top}, \tag{1}$$

where $\bar{X} = (\sum_1^N X_i)/N$ and $\bar{Y} = (\sum_1^N Y_i)/N$. We denote by Σ_{XX} (resp. Σ_{YY}) the covariance matrix of X (resp. Y): $\Sigma_{XX} = \mathrm{E}[(X-\bar{X})(X-\bar{X})^{\top}]$. The cross-covariance of X and Y is given by: $\Sigma_{XY} = \mathrm{E}[(X-\bar{X})(Y-\bar{Y})^{\top}]$. By further developing Eq. 1, one can write $\Lambda(X,Y)$ in a simpler way:

$$\Lambda(X,Y) = \begin{pmatrix} \Sigma_{XX} & \Sigma_{XY} \\ \Sigma_{YX} & \Sigma_{YY} \end{pmatrix}. \tag{2}$$

Λ is a $2d \times 2d$ matrix. It has the same properties as a classical covariance matrix: it is symmetric and positive definite. Then, we may also call Λ a tensor. In the 3D case, Λ is a 6×6 tensor.

2.2 Analysis of Total Covariance Matrices

In its current form, it is difficult to appreciate the meaning of the TCM and it cannot be easily represented (it is an ellipsoid in 6D). However, several matrix, vector and scalar measures may be derived from it. Here, we focus on quantifying the correlation of X and Y through the Canonical Correlation Analysis.

Canonical Correlation Analysis (CCA): CCA [3, 4] refers to the method of finding vector bases that maximize the correlation between two vector variates, and is the generalization of the correlation coefficient to multivariate data. In the scalar case, we define the correlation coefficient between x and y as: $\rho = \sigma_{xy}/\sqrt{\sigma_{xx}.\sigma_{yy}}$, where σ_{xx} (resp. σ_{yy}) is the variance of x (resp. y), and σ_{xy} is the cross-variance of x and y. Similarly, the correlation matrix Γ in the multivariate case is defined as:

$$\Gamma(X,Y) = \Sigma_{XX}^{-1/2}\Sigma_{XY}\Sigma_{YY}^{-1/2}. \tag{3}$$

We have the property that $\Gamma(Y,X) = \Gamma(X,Y)^\top$. Taking the mean trace of the Γ gives us an average correlation coefficient $\bar{\rho}$. The range of $\bar{\rho}$ lies between 0 (absence of correlation) and 1 (correlation). In multivariate statistics, however, a low average correlation coefficient may hide a potentially high correlation. This is the case, for instance, when only one component of X is correlated with one component of Y. Taking the average correlation coefficient may discard this relationship. To distinguish between correlations along potentially different axes, one needs to run a canonical correlation analysis, which is nothing else than decomposing Γ in singular values: $\Gamma = U.S.V^\top$, where U and V are orthogonal matrices of correlation vectors, and S is a diagonal matrix of correlation coefficients ρ_i.

Significance Testing: To test the statistical significance of the obtained correlations, [5] proposed to test the dimensionality of the correlation matrix. If its rank is zero, then there is no correlation ($\rho_i = 0, \forall i$). If we reject this hypothesis, then the rank is at least one, which means that at least two directions in space are correlated. We use the Bartlett-Lawley test [5] with the null hypothesis: $H_0 : \text{rank}(\Gamma) = 0$: $L(\Gamma) = -\left(N - d + \frac{1}{2}\right) \sum_{j=1}^{d} \log\left(1 - \rho_j^2\right)$. L's distribution is chi-squared under the Gaussian assumption on X and Y with d^2 degrees of freedom. We can consequently derive a p-value for testing the significance of correlations.

3 Experiments

We used a dataset of sulcal landmark curves manually delineated in 98 subjects by expert anatomists, according to a precise protocol with established reliability within and across raters [2]. The dataset consists of 47 men and 53 women (age: 51.8 +/- 6.2 years), all normal controls.The lines are traced in 3D on the cortical surface. We included the maximal subset of all curves that consistently appear in all normal subjects, 72 in total (36 per hemisphere). By repeated training, the maximum allowed inter- and intra-rater error (reliability) was ensured to be better than 2mm everywhere. MR images used for delineations were first linearly aligned to the ICBM stereotactic space [6].

We used the methodology outlined in [2] to determine the mean curve for each sulcal line by modeling samples as deformations of a single average curve. Mean curve computation involves filtering each sample by B-spline parameterization, minimization of total variance, and sulcal matching by dynamic programming.

In the following, we investigate the potential correlations between locations on different sulci. First, we study the correlation between particular sulcal lines and other cortical points not belonging to the same structure: we call this study *sulcal correlation*. Second, we assess *inter-hemispheric correlations* between corresponding anatomical points in the two hemispheres.

3.1 Sulcal Correlation for 6 Specific Positions

Methodology: Obviously, this study is a combinatorial challenge. We sampled the 72 mean sulci with approximately 500 points (average of 7 points per sulcus), which gives a total of

about 250000 pairs of points to process. To limit the number of pairs investigated, we focused on two major sulcal lines: the Central Sulcus (CS) and the Inferior Temporal Sulcus (ITS). The CS is a relatively stable landmark, dividing the frontal and parietal lobes, and separates primary sensory and motor cortices. The ITS is an important landmark in studies of facial imagery processing, as it separates the fusiform gyrus from the inferior temporal gyrus. These sulci lie in different lobes, develop at different times during gyrogenesis (CS developing earlier) and are distant in terms of fiber and functional connectivity, so they are good candidates for assessing inter-structure correlation, as little correlation is expected *a priori*. For each of these lines, three reference positions are picked: the beginning, middle, and end point. First, for each of the three reference positions, we extract the set of corresponding sulcal positions in each of the 98 subjects. Second, we compute the TCM of Eq. 2 with each of the remaining 499 average sulcal positions. We end up with a sparse field of TCMs. However, we would be more comfortable with a dense field of TCMs, as we could map those onto an average cortex to facilitate the visual interpretation of the results. We use Log-Euclidean (LE) metrics [7] and the methodology exposed in [2] (combination of a radial basis function interpolation with an harmonic partial differential equation) for extrapolating TCMs on a mean cortical surface. This type of interpolation was shown to preserve all the features of a covariance matrix, and has desirable properties like absence of swelling effect, and a smooth interpolation of the eigenvectors. Moreover, leave-one-out tests showed that this interpolation was able to predict missing data in regions locally correlated and is consequently well adapted for TCMs. The correlation matrix and the p-value derived from the CCA can now be computed at any point of the mean cortex. Notice that even if we only focused here on the p-value defined in Sec. 2.2, other measures are interesting, such as the principal vectors of correlation which are currently under investigation. This is why we need to extrapolate the full TCMs and not just the p-value.

The main problem for the curve matching procedure proposed in [2] is the *aperture problem*: correspondences in the direction tangent to the curve are almost impossible to retrieve without additional expert knowledge. To keep our results independent from this, we need to cancel the contribution in this tangential direction. The method proposed in this paper is the following. We define at each position of the mean sulci the Frenet frame, which gives us the plane orthogonal to the curve. Then, we project the sulcal positions onto this plane, which zeroes out the tangential component (see Fig. 1). Note that we lose one degree of freedom in the dimensionality of the data: vectors no longer have three degrees of freedom but two. This must be accounted for in the statistical tests of Sec. 2.2.

Results: p-value derived from the CCA are shown in Fig. 2. The significance level was set to 0.0001 to correct for multiple comparisons (Bonferroni correction applied on a threshold at 5% with 500 observations: $0.05/5000 = 0.0001$). A large area around the reference points shows high p-values: as expected, points that are anatomically close to the reference do have a correlated distribution among individuals. More interestingly, regions with high p-values most often include the structures' opposite hemisphere counterparts, but not always: the first (upper) and middle CS positions are highly correlated in the other hemisphere (Fig. 2 top panel, 1st and 2nd row), while the most inferior position is not, most likely because

its variability across subjects is extremely low (Fig. 2 top panel, 3rd row). In right-handed subjects, we know that some measures of motor skill (maximum finger tapping rate) correlate with gray matter volume positively in the left CS, but negatively in the right CS [8], which is reasonable given the left hemispheric specialization for fast repetitive movements in right-handers. Logically, such functional specializations may promote correlations between the two hemispheres in these regions of the CS, where tissue volumes directly correlate with skill levels. The posterior part of the ITS shows lowest correlation with its opposite hemisphere counterpart. Unlike the bottom of the CS, the posterior tip of the ITS is highly variable and asymmetric in structure and function - it is specialized for understanding the semantics of language in the left hemisphere, but for understanding prosodic aspects of language in the right hemisphere. This may suggest partially independent developmental programs for these functionally specialized structures. The long-range correlation between the back of the ITS and the left and right intra-parietal sulci is of interest, as the planum temporale and planum parietale are the two distinct areas most widely studied in neuroscience for their very high hemispheric asymmetry.

Nevertheless, it is intriguing that 5 of the 6 sulcal positions studied reflect a correlation with their symmetric counterpart in the opposite hemisphere. In the following, we test if this observation can be generalized to all sulcal positions.

3.2 Inter-Hemispheric Correlation Analysis

In this study, we specifically target the correlation between all points of one hemisphere and their homologous region in the other hemisphere. To do so, we first map all sulci of the right hemisphere onto the left. Then, we define a global mean, i.e. an average sulcal curve computed from the 98 left and right samples (Fig. 4). Global means provide a common reference curve to compare left and right positions. Correspondences between global means and left and right average curves are computed using the same framework as for the samples.

Figure 1: **Canceling the tangential component. Left:** Covariance matrices extracted along the mean Sylvian Fissure as in [2]. **Right:** The same tensors after canceling the tangential component. A small tangential value is kept for visualization purposes (tensors should be flat).

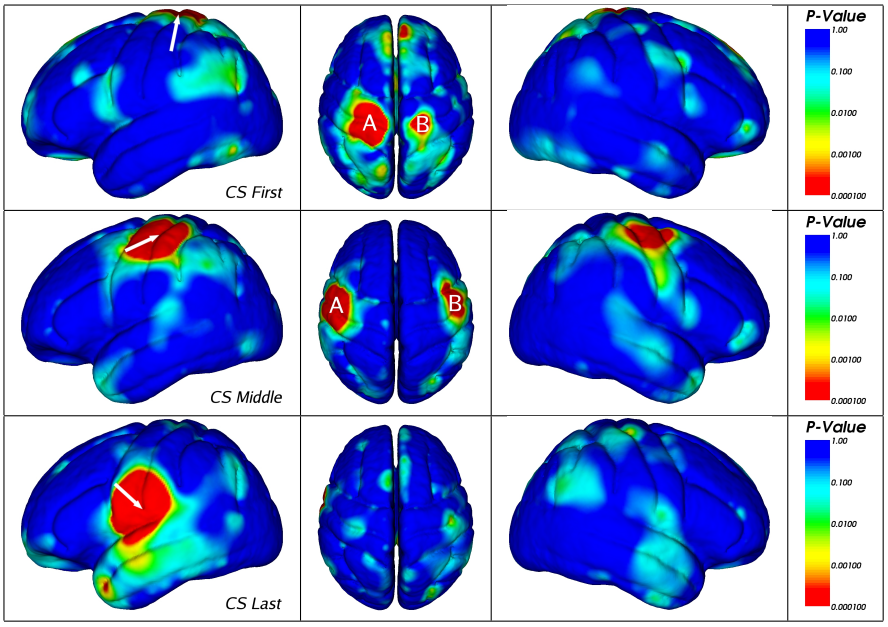

Figure 2: **Correlation Maps between Specific Reference Points and Other Brain Regions**. **Top panel: the Central Sulcus.** The significance level was set to 0.0001 for multiple comparisons correction. A white arrow in each row indicates a reference landmark; correlations with the reference landmark are plotted. Correlations for 3 reference landmarks on the CS are shown: the first (top row), the middle (second row), and the last, i.e. most inferior, position (third row) on the sulcal trace. Corresponding regions in the opposite hemisphere are highly correlated for the top and middle points (marked A and B). The lower end of the sulcus, however, exhibits low correlation with its symmetric contralateral counterpart.

For any given position on the global mean, we obtain corresponding points on left and right average curves, giving in turn correspondences between left and right sulcal positions in the 98 subjects (the choice of the left hemisphere is arbitrary, and we obtained the same results when using the right hemisphere instead). Finally, we compute the TCM of Eq. 2 between left and right positions. As for the sulcal correlation study, we extrapolate this sparse field of TCMs to an average left hemisphere surface, and cancel the tangential component which is consistently biased towards zero. Then, we extract p-values with the CCA and map those on the surface (Fig. 5). We apply the same Bonferroni correction as for the previous experiments and lower the significance level to 0.0001.

As observed previously on a few specific sulcal positions, most points are correlated with their symmetric counterparts. Regions with lowest correlations include Broca's and Wernicke's areas, which were already shown to exhibit the greatest asymmetries in variability [2]. These cortical regions are specialized for language production and comprehension respec-

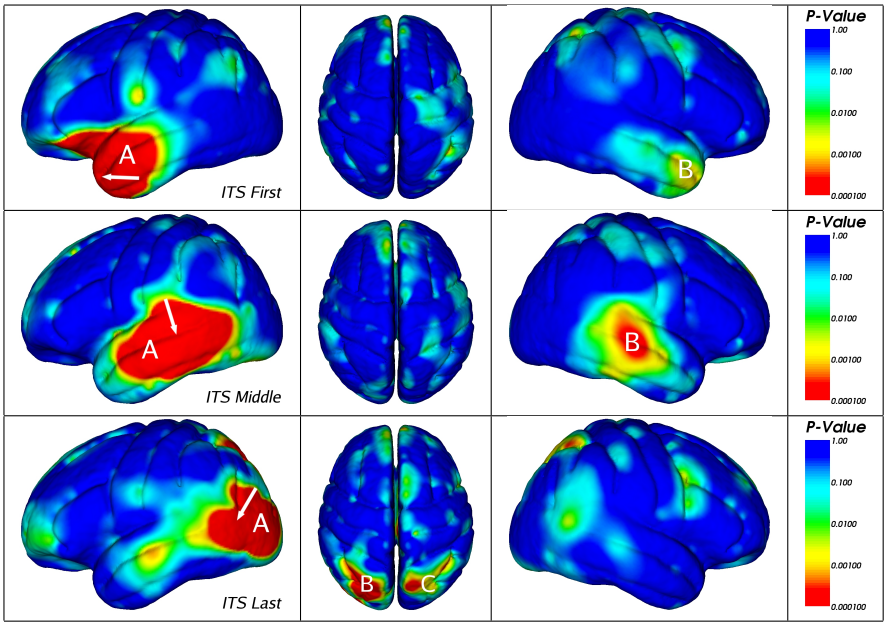

Figure 3: **Maps of Anatomical Correlation between Landmarks in the Perisylvian Language Cortex and other Brain Regions.** The significance level was set to 0.0001 for multiple comparisons correction. The same 3 positions as in Fig. 2 for the Inferior Temporal Sulcus are analyzed. The first (top row) and middle (second row) positions are symmetrically correlated (marks A and B). The last position (third row) correlates less with its opposite hemisphere counterpart, than with the intra-parietal sulci (marked B and C).

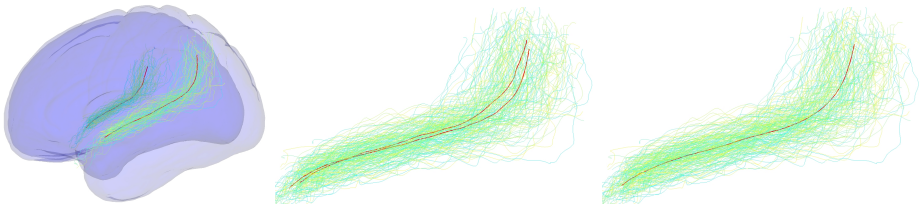

Figure 4: **Finding hemispheric correspondences.** The significance level was set to 0.0001 for multiple comparisons correction. **Left:** Positions of left and right Sylvian fissures (SF), in an oblique view, with a transparent cortical surface overlaid (in blue colors). **Middle:** All right hemisphere sulci are mapped to the left, including the two mean curves (in red). **Right:** Same set of sulci, whose global mean was computed and displayed in red. This is now used as a reference to compare left and right sulcal positions.

tively, but most right-handers show a greater reliance on the left hemisphere for language processing, and the volumes of these regions are highly asymmetric between hemispheres.

4 Conclusions and Perspectives

In this paper, we represent the cross-covariance between one point and any other point of the brain by a total covariance matrix describing not only the variability of the two points, but also their cross-covariance. Canonical correlation analysis allows us to test for the significance of these correlations. As TCMs have the same properties as classical covariance matrices (symmetric and positive-definite), we used the Log-Euclidean extrapolation to obtain a dense representation of initially sparsely-defined measures. This extrapolation was indeed previously shown to have good properties [2], contrary to the Euclidean extrapolation of the matrix coefficients.

We apply this method to study sulcal and hemispheric correlations. We showed that the central sulcus was highly correlated with its symmetric, except in its inferior part which is not highly variable. For the central sulcus, where motor skill is correlated with volume and is also lateralized, a strong hand preference for motor skills is likely to promote negative correlations between hemispheres for volumes in opposite regions. The Inferior Temporal Sulcus shows similar intriguing correlations, and its low correlation with its opposite counterpart may reflect their different developmental programs and functions.

Corresponding brain regions in each hemisphere are highly correlated, except for regions including Wernicke's and Broca's areas, which are known to be functionally specialized in one hemisphere. Any longer-range correlation - such as that found between the intra-parietal sulci and inferior temporal sulci - is in itself an interesting neuroscience finding. The planum

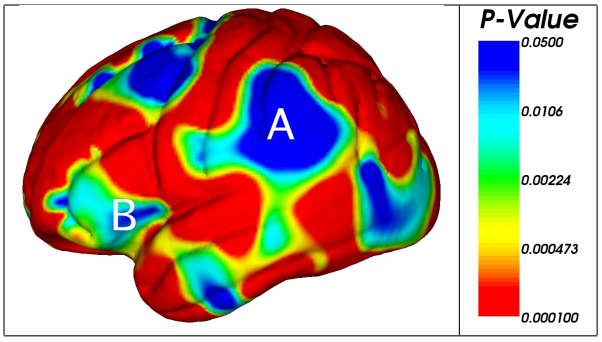

Figure 5: **Hemispheric correlations.** Hot colors (red) correspond to p-value$\leq$0.0001. Most of the cortex shows anatomical variantions that are correlated with their counterparts in the opposite hemisphere. Un-correlated regions include Wernicke's (marked A) and Broca's areas (marked B), which, in most subjects, are known to be more heavily specialized for language processing in the left hemisphere.

parietale and temporale are distinct highly asymmetric systems in each of these regions, and the long-range correlations may reflect common factors driving programmed asymmetries for both regions.

Future work includes a concrete modeling of these correlations. We could store, for each point of the brain, a minimal set of correlated positions, such as the local neighborhood and the set of distant most correlated points. This information could be used as a prior to guide inter-subject non-linear registration algorithms. Furthermore, a detailed study of all possible correlations between cortical landmarks could help understand the effects of genes on brain maturation. Validations of long-range correlations could be made using other sources of information, such as functional MRI: Are jointly activated regions, or causal models (achieved through structural equation modeling or dynamic causal modeling) for a given task related to anatomical correlations as well as connectivity (fiber bundle)? All this information, if it converges to the same outcome, could contribute to understanding the functional organization of the brain. Finally, these results should be compared with those of other methods, such as surface-based versus volumetric registration algorithms; this comparison is is currently underway for generating second-order models of brain variability [9].

References

[1] Mechelli, A., Friston, K.J., Frackowiak, R.S., Price, C.J.: Structural covariance in the human cortex. The Journal of Neuroscience **25**(36) (2005) 8303–8310

[2] Fillard, P., Arsigny, V., Pennec, X., Hayashi, K., Thompson, P., Ayache, N.: Measuring brain variability by extrapolating sparse tensor fields measured on sulcal lines. Neuroimage **34**(2) (2007) 639–650 Also as INRIA Research Report 5887, April 2006. PMID: 17113311.

[3] Hotelling, H.: Relations between two sets of variates. Biometrika **28** (1936) 231–377

[4] Rao, A., Babalola, K., Rueckert, D.: Canonical correlation analysis of sub-cortical brain structures using non-rigid registration. In: Proc. of WBIR. (2006)

[5] Fujikoshi, Y., Veitch, L.: Estimation of dimensionality in canonical correlation analysis. Biometrika **66**(2) (1979) 345–351.

[6] Collins, D., Holmes, C., Peters, T., Evans, A.: Automatic 3D model-based neuroanatomical segmentation. Human Brain Mapping **3**(3) (1995) 190–208

[7] Arsigny, V., Fillard, P., Pennec, X., Ayache, N.: Log-Euclidean metrics for fast and simple calculus on diffusion tensors. MRM **56**(2) (2006) 411–421

[8] Herve, P., Mazoyer, B., Crivello, F., Perchey, G., Tzourio-Mazoyer, N.: Finger tapping, handedness and grey matter amount in the rolando's genu area. NeuroImage **25**(4) (2005) 1133–45

[9] Durrlemann, S., Pennec, X., Trouvé, A., Ayache, N.: Measuring brain variability via sulcal lines registration: a diffeomorphic approach. In: Proc. of MICCAI'07. (2007) To appear.

Unité de recherche INRIA Sophia Antipolis
2004, route des Lucioles - BP 93 - 06902 Sophia Antipolis Cedex (France)

Unité de recherche INRIA Futurs : Parc Club Orsay Université - ZAC des Vignes
4, rue Jacques Monod - 91893 ORSAY Cedex (France)
Unité de recherche INRIA Lorraine : LORIA, Technopôle de Nancy-Brabois - Campus scientifique
615, rue du Jardin Botanique - BP 101 - 54602 Villers-lès-Nancy Cedex (France)
Unité de recherche INRIA Rennes : IRISA, Campus universitaire de Beaulieu - 35042 Rennes Cedex (France)
Unité de recherche INRIA Rhône-Alpes : 655, avenue de l'Europe - 38334 Montbonnot Saint-Ismier (France)
Unité de recherche INRIA Rocquencourt : Domaine de Voluceau - Rocquencourt - BP 105 - 78153 Le Chesnay Cedex (France)

Éditeur
INRIA - Domaine de Voluceau - Rocquencourt, BP 105 - 78153 Le Chesnay Cedex (France)
http://www.inria.fr
ISSN 0249-6399